

Effects of collisions and saturation on multiphoton processes and nonlinear mixing in the field of two pumps

G. S. Agarwal and N. Nayak

School of Physics, University of Hyderabad, Hyderabad 500134, Andhra, India

(Received 6 May 1985)

The nonlinear response of a two-level system interacting with two pump beams of different frequencies is studied with a view to examine several recent experiments on nonlinear mixing of high orders, instabilities in homogeneously broadened lasers, and holes in homogeneous lines. Such a nonlinear response is calculated with use of the continued fractions given in our earlier work [J. Opt. Soc. Am. **B1**, 164 (1984)]. Saturation effects lead to the appearance of many structures at submultiples of the Rabi frequency. The origin of these subharmonics in nonlinear-response functions is explained. It is shown that collisions not only lead to hole burning at the line center for weak fields but can also lead in moderate fields to the appearance of structures at subharmonics of the Rabi frequency. Existence of collision-induced coherences similar to those in four-wave mixing is shown in six-wave mixing. Exact results for the degenerate nonlinear mixing of arbitrary order are presented for arbitrary values of field strengths. Saturating fields create holes at the line center of such nonlinear mixing signals. Gain profiles of two modes symmetrically displaced from line center are also given. Numerical results, with complete account of saturation and collisions, for a variety of nonlinear-response functions are presented.

I. INTRODUCTION

A very large number of physical phenomena in the resonant interaction of atomic-molecular systems with radiation fields can be studied by treating the atomic system as a two-level system and by examining its response to applied fields.¹ Various perturbative results are well known.²⁻⁶ If one of the applied fields is strong, then a number of nonperturbative results can also be obtained.⁷⁻¹⁴ A number of recent experimental works¹⁵⁻¹⁸ require knowledge of the nonperturbative response functions, when both the applied fields are strong. These include a variety of nonlinear mixing^{15,16} experiments, where not only four-wave mixing but also higher-order mixing in saturating fields has been studied. Similarly, conventional pump-probe experiments have been repeated¹⁸ with probes whose intensity could be large. Experiments on instabilities in lasers involving the switching from a single mode to, for example, two-mode operation also necessitate the exact solution in the presence of two strong fields. The purpose of this paper is to formulate the general theory and to use it to understand some of these experiments. We will also carry out detailed investigations on the effect of collisions since collisions are known to change the spectral line shapes in a manner which in many cases is very different from a simple broadening of the spectral line. The effects are particularly more dramatic in nonlinear spectroscopy; for example, collisions are responsible for the appearance of additional resonances^{19,20} in four-wave mixing. Collisions also lead to spectral hole burning²¹ in homogeneous probe line shapes in the presence of a pump. The interesting cases invariably involve the interaction of two or more fields with the system. The previous studies have concentrated mostly on results obtained by using third-order perturba-

tion theory. Obviously the effect of collisions on results obtained beyond perturbation theory will be quite interesting.

In a recent paper to be referred to as I, we studied the dynamical behavior of a two-level system interacting with two strong fields.²² We showed how nonlinear susceptibilities to all orders in the fields can be obtained by the numerical solution of a continued fraction. It may be added that Toptygina and Fradkin¹⁸ perhaps used the continued fractions for the first time to explain the experimental results¹⁸ of Bonch-Bruevich *et al.* on energy absorption in strong fields. Our work concerns mostly higher-order nonlinear mixing process in two saturating fields. The development of paper I is especially suited for studying the effects of collisions on multiphoton processes in the presence of two pump waves. In the present paper we investigate in detail the effects of collisions and saturation on a variety of nonlinear-response functions. In Sec. II we recall the basic equations that yield the nonlinear response of a two-level system in two intense fields. We also outline the derivation of the perturbative results when one field is weak and the other could be intense. Such perturbative results clearly show how the resonances at subharmonics of the Rabi frequency arise as the strength of the weak field is increased. In Sec. III we investigate the nonlinear response at one of the applied frequencies. The recursion relation for the Fourier components of the atomic inversion enables us to understand the origin of various terms in the nonlinear susceptibility. When both the fields are of moderate intensity, then additional resonances in the response function can be induced by collisions. In Sec. IV we present exact results for the susceptibilities describing nonlinear mixing of arbitrary order. Saturation leads to holes at the line center in these susceptibilities. In Sec. V we examine the saturation effects in

four-wave mixing. Asymmetries with regard to the strength of the two fields are discussed. In Sec. VI we show the existence of collision-induced coherences in fifth-order susceptibility. This susceptibility exhibits the resonances at the subharmonic of the Rabi frequency even in the case when only one field is strong. Finally in Sec. VII we discuss gain profiles of two modes symmetrical about the line center. Such gains have been recently studied in connection with instabilities in homogeneously broadened lasers.

II. NONLINEAR-RESPONSE EQUATIONS IN TWO INTENSE FIELDS

We first recall the basic equations from I. The Bloch equations in the frame rotating with frequency ω_2 of the field \mathcal{E}_2 for a two-level system in the presence of two intense fields $\mathcal{E}_1, \mathcal{E}_2$ read

$$\dot{\underline{\psi}} = \underline{A}\underline{\psi} + \underline{I} + \underline{B}_+ e^{i\Omega t} \underline{\psi} + \underline{B}_- e^{-i\Omega t} \underline{\psi}, \quad (2.1)$$

where

$$\underline{\psi} = \begin{pmatrix} e^{-i\omega_2 t} \rho_{21} \\ e^{i\omega_2 t} \rho_{12} \\ (\rho_{11} - \rho_{22})/2 \end{pmatrix}, \quad (2.2)$$

$$\underline{A} = \begin{pmatrix} i\Delta_2 - \frac{1}{T_2} & 0 & 2i\mathbf{d} \cdot \mathcal{E}_2^* \\ 0 & -i\Delta_2 - \frac{1}{T_2} & -2i\mathbf{d} \cdot \mathcal{E}_2 \\ i\mathbf{d} \cdot \mathcal{E}_2 & -i\mathbf{d} \cdot \mathcal{E}_2^* & -\frac{1}{T_1} \end{pmatrix},$$

$$\Delta_2 = \omega_0 - \omega_2, \quad \Omega = \omega_1 - \omega_2. \quad (2.3)$$

The nonvanishing elements of \underline{B}_\pm are

$$\begin{aligned} (\underline{B}_+)_{13} &= 2i\mathbf{d} \cdot \mathcal{E}_1^*, & (\underline{B}_-)_{23} &= -2i\mathbf{d} \cdot \mathcal{E}_1, \\ (\underline{B}_+)_{32} &= -i\mathbf{d} \cdot \mathcal{E}_1^*, & (\underline{B}_-)_{31} &= i\mathbf{d} \cdot \mathcal{E}_1, \end{aligned} \quad (2.4)$$

$$\underline{I}_3 = \eta \equiv (\rho_{11}^{(0)} - \rho_{22}^{(0)})/2T_1.$$

In Eqs. (2.2), T_1 and T_2 are the longitudinal and transverse relaxation times, ω_0 is the frequency of the two-level system, \mathbf{d} is the dipole matrix element assumed to be real and $\rho_{ii}^{(0)}$ represents the equilibrium population of the level $|i\rangle$. The fields are assumed to be monochromatic and nonfluctuating. The steady-state solution of (2.1) has been shown to be

$$\underline{\psi} = \sum_{-\infty}^{+\infty} \underline{\psi}^{(n)} e^{-in\Omega t}, \quad (2.5)$$

where

$$\underline{\psi}_1^{(n)} = (2ig_2 \underline{\psi}_3^{(n)} + 2ig_1 \underline{\psi}_3^{(n+1)})/D_n, \quad (2.6)$$

$$\underline{\psi}_2^{(n)} = -(2ig_2 \underline{\psi}_3^{(n)} + 2ig_1 \underline{\psi}_3^{(n-1)})/D_{-n}^*, \quad (2.7)$$

and where

$$D_n = \frac{1}{T_2} - i\Delta_2 - in\Omega.$$

Here $\underline{\psi}_3^{(n)}$'s are to be obtained from the recursion relation

$$a_n X_n + b_n X_{n+1} + c_n X_{n-1} = \eta \delta_{n0}, \quad X_n \equiv \underline{\psi}_3^{(n)}, \quad (2.8)$$

$$\begin{aligned} b_n &= 2g_1 g_2 \left[\frac{1}{D_n} + \frac{1}{D_{-n-1}^*} \right], \\ c_n &= 2g_1 g_2 \left[\frac{1}{D_{n-1}} + \frac{1}{D_{-n}^*} \right], \quad g_i = \mathbf{d} \cdot \mathcal{E}_i, \end{aligned} \quad (2.9)$$

$$a_n = \frac{1}{T_1} - in\Omega + \frac{2g_2^2}{D_{-n}^*} + \frac{2g_1^2}{D_{n-1}} + \frac{2g_1^2}{D_{-n-1}^*} + \frac{2g_2^2}{D_n}. \quad (2.10)$$

The solution of (2.8) can be obtained from the continued fraction

$$X_0 = \eta [a_0 + 2 \operatorname{Re}(b_0 Y_1)]^{-1}, \quad Y_n = X_n / X_{n-1}, \quad n \neq 0 \quad (2.11)$$

$$Y_n = -c_n (a_n + b_n Y_{n+1})^{-1}.$$

The induced polarization P is related to $\underline{\psi}$'s by

$$\mathbf{P} = \mathbf{d}[\rho_{12}(t) + \rho_{21}(t)] = \mathbf{d}[e^{i\omega_2 t} \underline{\psi}_1(t) + \text{c.c.}],$$

which can be written as

$$\mathbf{P}(t) = \mathbf{d} \left[\sum_n \underline{\psi}_1^{(n)} e^{-in(\omega_1 - \omega_2)t + i\omega_2 t} + \text{c.c.} \right]. \quad (2.12)$$

From (2.12), the nonlinear susceptibilities of various orders can be calculated. Note that $\underline{\psi}_1^{(n)}$'s depend on all powers of g_1 and g_2 . Perturbative expressions can be obtained by expanding $\underline{\psi}_1^{(n)}$ in various orders in g_1 and g_2 . The response at the frequency $(n+1)\omega_2 - n\omega_1$ is given by $(\underline{\psi}_1^{(n)})^* \equiv \underline{\psi}_2^{(-n)}$, whereas the response at $n\omega_1 - (n-1)\omega_2$ is given by $\underline{\psi}_1^{(n)}$. The recursion relation (2.8) is very useful in obtaining perturbative results as shown below and in subsequent sections.

Since there are two perturbation parameters, we therefore write X_n as

$$X_n = \sum_{\mu, \nu=0}^{\infty} X_n^{(\mu, \nu)} g_1^\mu g_2^\nu, \quad (2.13)$$

which can also be written in the forms

$$X_n = \sum_{\nu=0}^{\infty} B_n^{(\nu)} g_2^\nu = \sum_{\mu=0}^{\infty} A_n^{(\mu)} g_1^\mu. \quad (2.14)$$

Thus $X_n^{(\mu, \nu)}$ represents the contribution of order $g_1^\mu g_2^\nu$, whereas $B_n^{(\nu)}$ ($A_n^{(\mu)}$) represents the contribution to all orders in g_1 (g_2) but to order ν (μ) in g_2 (g_1). From (2.7) and (2.12) the response at $\omega_2 + n(\omega_2 - \omega_1)$ is

$$R(\omega_2(n+1) - n\omega_1) = (-2ig_2 X_{-n} - 2ig_1 X_{-n-1})/D_n^*, \quad (2.15)$$

the perturbative expressions for which can be obtained from (2.13) and (2.14). Writing a_n , b_n , and c_n as

$$a_n = (\alpha_n + g^2 f_n + g^2 h_n), \quad b_n = g_1 g_2 \beta_n, \quad (2.16)$$

$$c_n = g_1 g_2 \gamma_n,$$

the recursion relation (2.8) leads to

$$\alpha_n X_n^{(\mu, \nu)} + f_n X_n^{(\mu-2, \nu)} + h_n X_n^{(\mu, \nu-2)} + \beta_n X_{n+1}^{(\mu-1, \nu-1)} + \gamma_n X_{n-1}^{(\mu-1, \nu-1)} = \eta \delta_{n0} \delta_{\mu 0} \delta_{\nu 0}. \quad (2.17)$$

Similarly, the perturbative expressions for $B_n^{(\nu)}, A_n^{(\mu)}$ are

$$(\alpha_n + g^2 f_n) B_n^{(\nu)} + h_n B_n^{(\nu-2)} + g_1 \beta_n B_{n+1}^{(\nu-1)} + g_1 \gamma_n B_{n-1}^{(\nu-1)} = \eta \delta_{n0} \delta_{\nu 0}, \quad (2.18)$$

$$(\alpha_n + g^2 h_n) A_n^{(\mu)} + f_n A_n^{(\mu-2)} + g_2 \beta_n A_{n+1}^{(\mu-1)} + g_2 \gamma_n A_{n-1}^{(\mu-1)} = \eta \delta_{n0} \delta_{\mu 0}. \quad (2.19)$$

Thus the response to the desired order can be obtained by using either of the above three equations. For example, from (2.18) we get

$$B_n^{(0)} = (\alpha_n + g^2 f_n)^{-1} \eta \delta_{n0}, \quad (2.20)$$

$$B_n^{(1)} = -(\alpha_n + g^2 f_n)^{-1} (g_1 \beta_n B_{n+1}^{(0)} + g_1 \gamma_n B_{n-1}^{(0)}) = -(\alpha_n + g^2 f_n)^{-1} \eta (\alpha_0 + g^2 f_0)^{-1} (g_1 \beta_n \delta_{n,-1} + g_1 \gamma_n \delta_{n1}), \quad (2.21)$$

$$B_n^{(2)} = -(\alpha_n + g^2 f_n)^{-1} [h_n B_n^{(0)} + g_1 \beta_n B_{n+1}^{(1)} + g_1 \gamma_n B_{n-1}^{(1)}] = -(\alpha_n + g^2 f_n)^{-1} \eta (\alpha_0 + g^2 f_0)^{-1} [h_n \delta_{n0} - g_1 (\alpha_{n+1} + g^2 f_{n+1})^{-1} \beta_n (g_1 \beta_{n+1} \delta_{n+1,-1} + g_1 \gamma_{n+1} \delta_{n+1,1}) - g_1 (\alpha_{n-1} + g^2 f_{n-1})^{-1} \gamma_n (g_1 \beta_{n-1} \delta_{n-1,-1} + g_1 \gamma_{n-1} \delta_{n-1,1})]. \quad (2.22)$$

The quantities $A_n^{(\mu)}$ can be obtained from the above by the replacements $g_1 \rightarrow g_2, f_n \rightarrow h_n, h_n \rightarrow f_n$. The denominators which appear in (2.22) play a very important role in the studies of the effects of saturation. On using the definition of D 's, we find that

$$\alpha_n + g^2 f_n = \left[\frac{1}{T_2} - i\Delta_1 + z \right]^{-1} \left[\frac{1}{T_2} + i\Delta_1 + z \right]^{-1} P_1(z), \quad z = -in\Omega, \quad \Delta_1 = \omega_0 - \omega_1 = \Delta_2 - \Omega, \quad (2.23)$$

where

$$P_1(z) = \left[z + \frac{1}{T_1} \right] \left[z + \frac{1}{T_2} - i\Delta_1 \right] \left[z + \frac{1}{T_2} + i\Delta_1 \right] + 4g_1^2 \left[z + \frac{1}{T_2} \right]. \quad (2.24)$$

The roots of the polynomial (2.24) determine, among other things, dynamic Stark splittings.^{1,7,8} Note that calculations in higher orders involve not only $P(-i\Omega)$ but also $P(-2i\Omega)$, etc. Thus not only will the response functions show the usual Stark splittings but also the splittings at the subharmonics of the Rabi frequency. Our numerical results in Ref. 22 indeed show these subharmonics.²³

III. RESPONSE FUNCTIONS AT THE APPLIED FREQUENCIES

In this section we investigate the structure of the response function at one of the applied frequencies, say ω_2 . This function $R(\omega_2)$ in the lowest order in g_2 but to all orders in g_1 is very well known.⁷ The analysis based on (2.6)–(2.8) sheds new light on the various processes that contribute to such a response. Using (2.15) and (2.14), we find to first order in g_2 and to all orders in g_1

$$R^{(\infty, 1)}(\omega_2) = (-2ig_2 B_0^{(0)} - 2ig_1 g_2 B_{-1}^{(1)}) / D_0^*. \quad (3.1)$$

From (2.20) and (2.23), the contribution $B_0^{(0)}$ is

$$B_0^{(0)} = \eta \left[\left[\frac{1}{T_2} \right]^2 + \Delta_1^2 \right] \left[\frac{1}{T_1} \right] \left[\left[\frac{1}{T_2} \right]^2 + \Delta_1^2 + 4 \frac{g_1^2}{T_2} \right]^{-1}. \quad (3.2)$$

Note that physically $B_0^{(0)}$ represents the inversion in the two-level medium in the absence of the g_2 field but in the presence of the saturating field g_1 . The contribution proportional to $B_0^{(0)}$ has been referred to as that arising from the sequential absorption.⁵ The term $B_{-1}^{(1)}$ is equal to

$$B_{-1}^{(1)} = -\eta (\alpha_{-1} + g^2 f_{-1})^{-1} (\alpha_0 + g^2 f_0)^{-1} g_1 \beta_{-1},$$

which on using (2.23) reduces to

$$B_{-1}^{(1)} = -2\eta T_1 \left[\left[\frac{1}{T_2} \right]^2 + \Delta_1^2 \right] \left[\left[\frac{1}{T_2} \right]^2 + \Delta_1^2 + 4 \frac{T_1}{T_2} g_1^2 \right]^{-1} g_1 \times \left[\left[\frac{1}{T_2} + i\Omega \right]^2 + \Delta_1^2 \right] P^{-1}(i\Omega) \left[\left[\frac{1}{T_2} - i\Delta_1 \right]^{-1} + \left[\frac{1}{T_2} + i\Delta_2 \right]^{-1} \right]. \quad (3.3)$$

It is also interesting to note that the Rabi structures in the response function $R^{(\infty,1)}(\omega_2)$ arise from the contribution coming from $B_{-1}^{(1)}$ terms. Hence it is clear that if one had retained only the contribution coming from the sequential absorption term, then the resonances at the Rabi frequen-

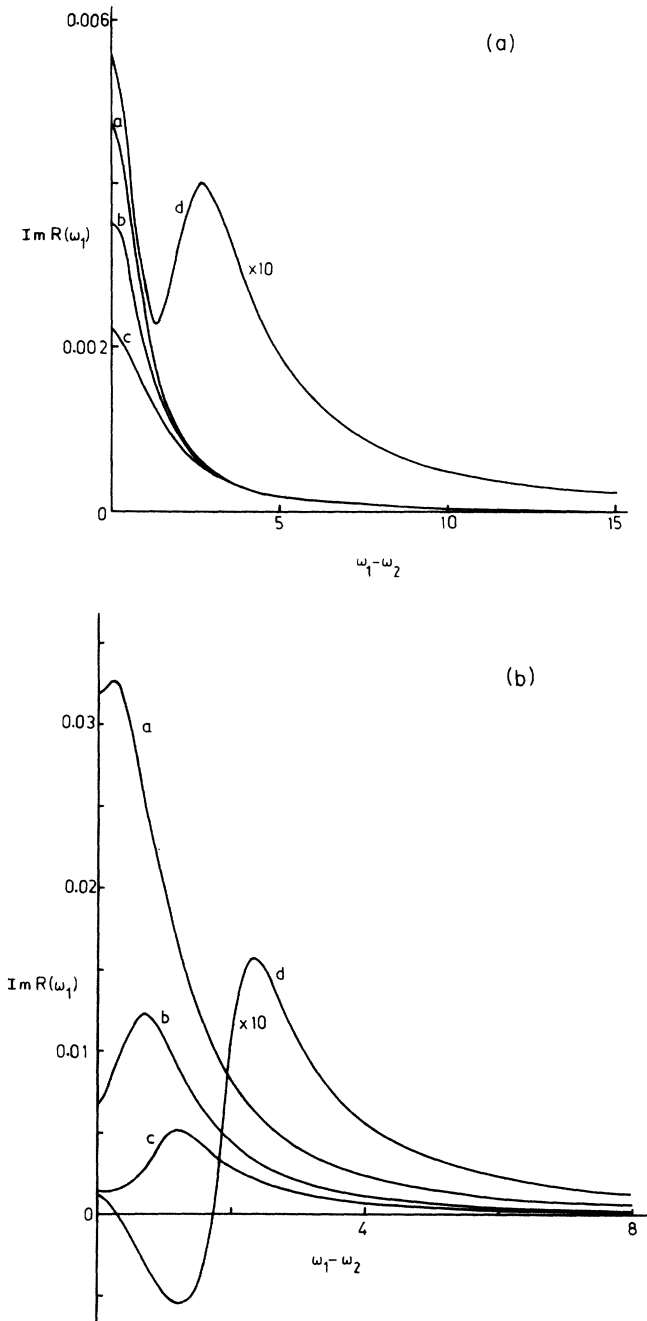


FIG. 1. Energy absorption from the weak field 1 [which is proportional to $\text{Im}R(\omega_1)$] as a function of $\omega_1 - \omega_2$ when the second field is on resonance with the atomic transition frequency. g_2 values for the curves *a*, *b*, *c*, and *d* are, respectively, 0.1, 0.3, 0.5, and 1.0. All parameters are in units of $1/T_2$. (a) is for radiative relaxation. The effects of collisions are shown in (b).

cy would have been missed. Moreover, for strong fields the term $B_{-1}^{(1)}$ gives the dominant contribution in the resonance region. This can, for example, be seen easily in the special case $\Delta_1 = 0$. The contribution from the term $B_{-1}^{(1)}$ can be interpreted as follows: the simultaneous action of the two fields produces a population grating (in time) in the medium, i.e., produces a beat frequency $(\omega_1 - \omega_2)$ at which the population oscillates. Such an oscillation combines with the coherent oscillation of the dipole moment at the frequency ω_1 produced by the field g_1 which results in the response at ω_2 . There is a special case when g_1 is set to zero in the denominators in (3.3); such a contradiction has been discussed by Boyd and Mukamel.⁵ Boyd and Mukamel also pointed out that the presence of collisions ($1/T_1 \neq 2/T_2$) can lead to a hole in the homogeneous line. They examined the response $R^{(2,1)}(\omega_2)$ to order $g_2^2 g_1$ and found that the resonant structure at the origin starts showing a dip as the pressure is increased.²¹ While Boyd and Mukamel restricted their analysis to lowest order in g_1 and g_2 , it is now possible, using the present formulation, to examine the interplay of collisional and saturation effects. For this purpose (2.15) is used and the continued fraction is numerically evaluated. The results for the energy absorption from field 1 over a very wide range of field strengths and collisional parameters are shown in Figs. 1–3. In Fig. 1, the field ω_2 is taken to be on resonance with the medium transition and its strength is weak whereas the strength of the field ω_1 is varied from low values to moderate values. The results are shown as a function of $\omega_1 - \omega_2$, i.e., the absorption is studied as a function of ω_1 . Figure 1(a) is for radiative relaxation whereas Fig. 1(b) shows the results when the collisions are dominant. On comparison of Figs. 1(a) and 1(b), we see the hole burnt at $\omega_1 - \omega_2 = 0$ in the case when collisions are dominant and when the fields are weak. For moderate field strength g_2 ($g_2 \sim 1$) the absorption profile with collisions acquires dispersive structure and regions of amplifications appear, which is in contrast to the results for radiative case. It must be remembered that all the parameters are in units of $1/T_2$ and since T_2 is different in the two cases, the given values of g_2 imply fields with different field strengths. Of course, a field is referred to as weak or strong if the corresponding Rabi frequency is much less or bigger than $1/T_2$. In Fig. 2, we present the results for absorption from field 1 for moderate strengths. The strength of field 2 is changed from low to high values. For low strengths g_2 , one again has the hole burning for the collisional case. For moderate values of g_2 , additional features (curves marked *b*) start appearing if collisions are taken into account. Thus collisions can lead to the appearance of the structures at the subharmonics.

IV. EXACT RESULTS FOR SUSCEPTIBILITIES FOR HIGHER-ORDER NONLINEAR MIXING OF FIELDS WITH EQUAL FREQUENCIES

As another application of the formalism of Sec. II, we consider nonlinear mixing^{15,16,19,24} of two fields with wave vectors \mathbf{k}_1 and \mathbf{k}_2 which are almost colinear. We consider

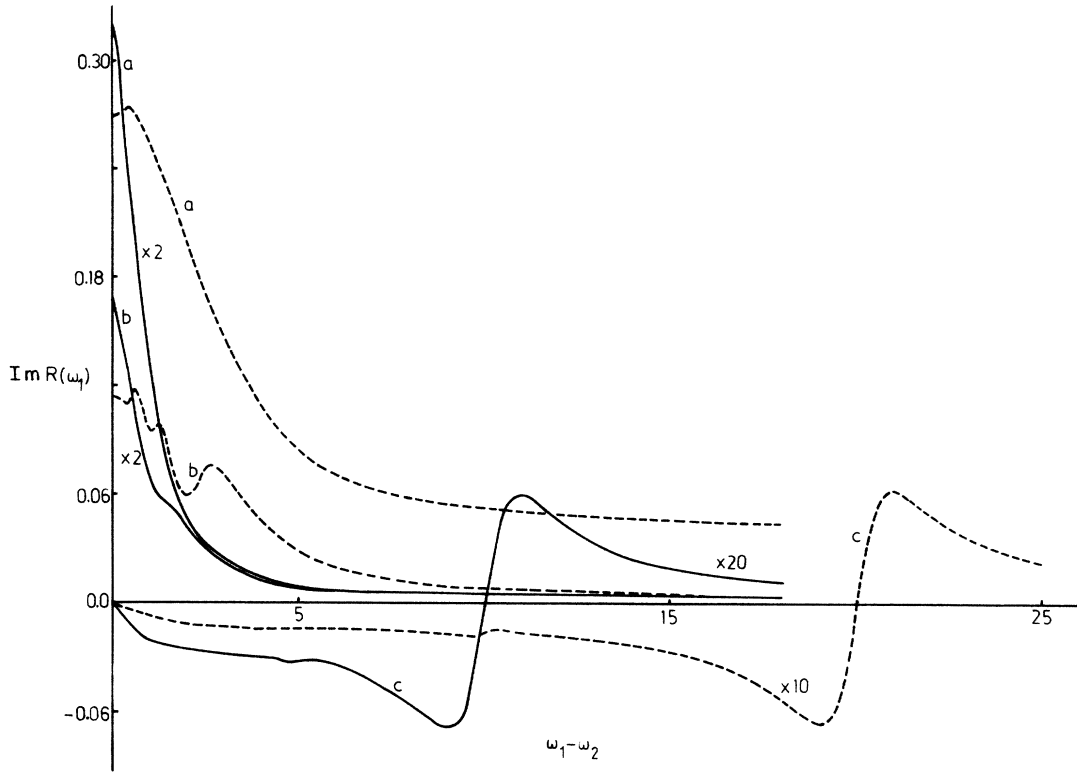


FIG. 2. Same as in Fig. 1 but now field 1 is of moderate strength, $g_1 = 1.0$. Dashed (solid) curves are for the case of collisional (radiative) relaxation. Note the appearance of collisionally induced coherences for $g_2 = 1$. Curves a , b , and c correspond, respectively, to $g_2 = 0.5, 1.0$, and 10 . The actual scale on x axis for solid curves is twice that shown.

the degenerate case, i.e., assume that the two fields have the same frequency. One can produce coherent radiation in the direction, say, $\mathbf{k}_2 + n(\mathbf{k}_2 - \mathbf{k}_1)$, and at frequency ω . In fact, in the experiments¹⁵ of Tan-no *et al.* nonlinear mixing up to 27th order [i.e., in the direction $\mathbf{k}_2 + 13(\mathbf{k}_2 - \mathbf{k}_1)$] was observed. It is clear from (2.12) that the induced polarization leading to coherent radiation in the direction $\mathbf{k}_2 + n(\mathbf{k}_2 - \mathbf{k}_1)$ will be determined by $\psi_1^{(n)*}$. The intensity $S_{-n,n+1}$ of the coherent radiation in this direction will be proportional to

$$S_{-n,n+1} = |\psi_1^{(n)*}|^2. \quad (4.1)$$

We will now show that the exact expression for $S_{-n,n+1}$ valid to all orders in g_1 and g_2 can be obtained. From (2.6) we have, by setting $\Omega = 0$,

$$\psi_1^{(n)} = (2ig_2X_n + 2ig_1X_{n+1})/D, \quad D \equiv \frac{1}{T_2} - i\Delta_2. \quad (4.2)$$

For $\Omega = 0$, the continued fraction can be summed up exactly leading to

$$Y_1 = -\frac{a}{2b} \left[1 - \left[1 - \frac{4b^2}{a^2} \right]^{1/2} \right], \quad (4.3)$$

$$X_0 = \frac{\eta}{a} \left[1 - \frac{4b^2}{a^2} \right]^{-1/2},$$

$$a = \frac{1}{T_1} + \frac{4(g_1^2 + g_2^2)}{T_2 \left[\Delta_2^2 + \left[\frac{1}{T_2} \right]^2 \right]}, \quad (4.4)$$

$$b = c = \frac{4g_1g_2}{T_2 \left[\Delta_2^2 + \left[\frac{1}{T_2} \right]^2 \right]}.$$

Each higher-order Y and X can be calculated from the lower orders

$$Y_{n+1} = -\frac{1}{b} \left[a + \frac{c}{Y_n} \right], \quad (4.5)$$

$$X_{n+1} = Y_{n+1}Y_nY_{n-1} \cdots Y_1X_0. \quad (4.6)$$

In fact, on combining (4.3)–(4.6) we find the important result

$$Y_n = Y_1 \quad \forall n, \quad X_n = (Y_1)^n X_0, \quad (4.7)$$

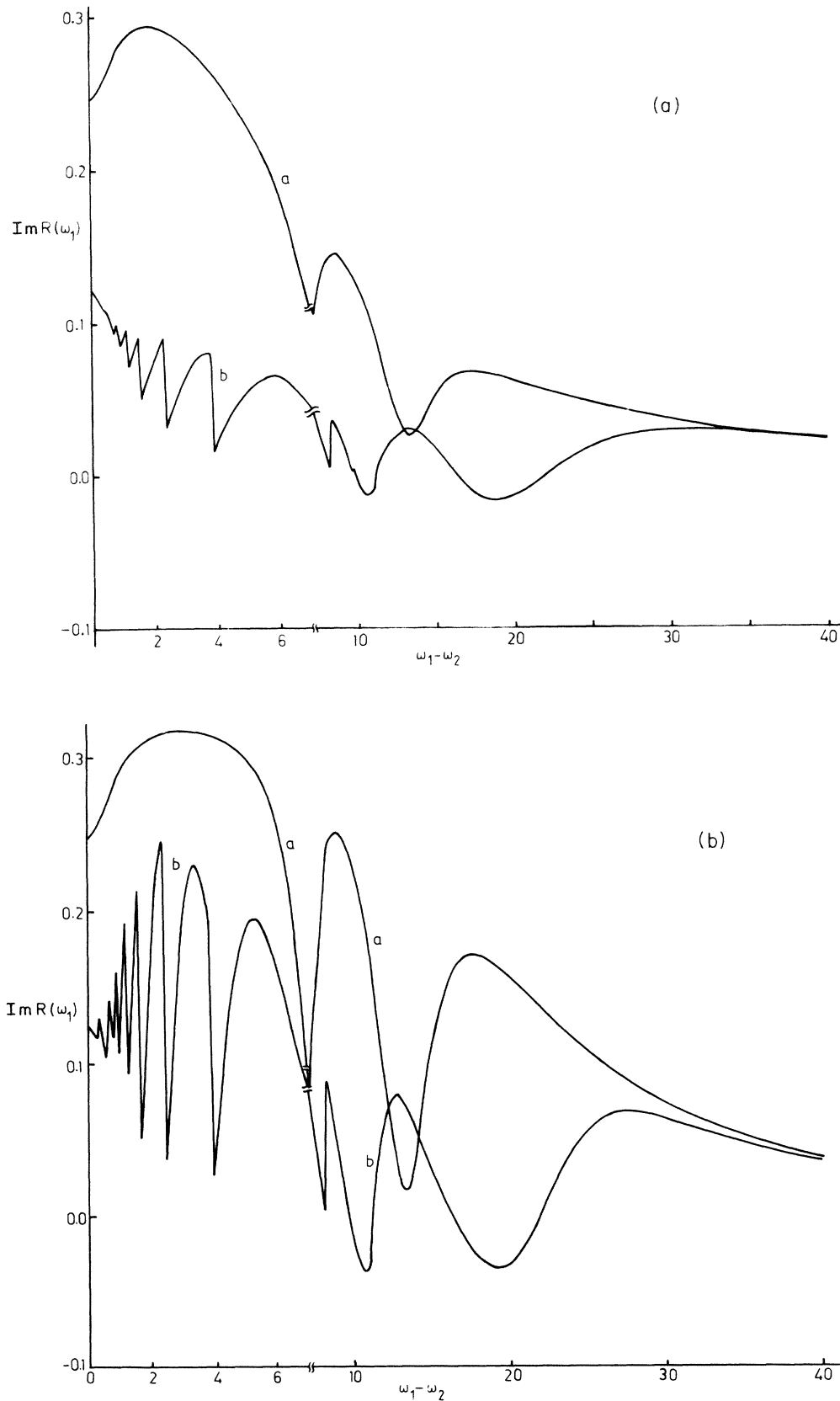


FIG. 3. (a) Same as in Fig. 1 but now field 1 is strong $g_1 = 10$, g_2 values are (a) 5, (b) 10, and $1/T_1 = 2/T_2 = 2$. Note the appearance of the resonances at subharmonics of the Rabi frequency. (b) Same as (a) but for collisional relaxation.

and hence the final expression for the coherent signal is

$$S_{-n,n+1} = \frac{4}{\left[\left(\frac{1}{T_2} \right)^2 + \Delta_2^2 \right]} |g_2 + g_1 Y_1|^2 |Y_1^{2n}| |X_0^2|. \quad (4.8)$$

The expression (4.8) is valid to all orders²⁵ in g_1 and g_2 . It is also an asymmetric function of g_1 and g_2 . Note that the lowest-order perturbation result will be proportional to $g_2^2 |g_1 g_2|^{2n}$. On further simplification we find that

$$Y_1 = -8g_1 g_2 / [\mu + (\mu^2 - 64g_1^2 g_2^2)^{1/2}], \quad (4.9)$$

$$X_0 = \eta T_2 \left[\left(\frac{1}{T_2} \right)^2 + \Delta_2^2 \right] / (\mu^2 - 64g_1^2 g_2^2)^{1/2}, \quad (4.10)$$

$$\mu = 4(g_1^2 + g_2^2) + \left[\frac{T_2}{T_1} \right] \left[\Delta_2^2 + \left(\frac{1}{T_2} \right)^2 \right]. \quad (4.11)$$

Note that Y_1 is at least of order $g_1 g_2$. The lowest perturbative result is now easily found

$$S_{-n,n+1} = \frac{g_2^{2n+2} g_1^{2n} (\eta T_1)^2 (4)^{2n+1} \left[\frac{T_1}{T_2} \right]^{2n}}{\left[\Delta_2^2 + \left(\frac{1}{T_2} \right)^2 \right]^{2n+1}} \left[\frac{T_1}{T_2} \right]^{2n} + \dots, \quad (4.12)$$

where the ellipsis includes the unspecified higher-order terms. It is interesting to note that the linewidth of the signal is less than $1/T_2$, with width decreasing as n increases. Similar reduction²⁵ in the linewidth has been predicted in modulation experiments.

The effect of saturation in generation of the coherent radiation in the direction $\mathbf{k}_2 + n(\mathbf{k}_2 - \mathbf{k}_1)$ is shown in Figs. 4 and 5, where we have plotted (4.8) for a range of g_1 and g_2 values. We only display the results for four- and six-wave mixings. In the lowest order of perturbation theory the term

$$\left| 1 + \frac{g_1 Y_1}{g_2} \right| = \left| 1 - \frac{8g_1}{\mu + (\mu^2 - 64g_1^2 g_2^2)^{1/2}} \right| \approx 1$$

and one has a resonant structure at $\Delta_2 = 0$. When saturation effects are accounted for, then $|1 + g_1 Y_1/g_2|$ becomes small, i.e., it exhibits a minimum at $\Delta_2 = 0$. In fact, at $\Delta_2 = 0$ and for large g_1, g_2

$$\left| 1 + \frac{g_1 Y_1}{g_2} \right| = \begin{cases} 0 & \text{if } g_1 > g_2, \\ (1 - g_1^2/g_2^2) & \text{if } g_1 < g_2. \end{cases} \quad (4.13)$$

This explains the bell-shaped structures of Figs. 4 and 5 and the dip at the origin for large field strengths. Recent experiments¹⁶ have in fact seen such structures in the case of nonlinear mixing of counterpropagating fields with large strengths. Our exact results of this section show how the peak $\Delta_2 = 0$ in weak fields transforms into a bell-shaped structure for intense fields.

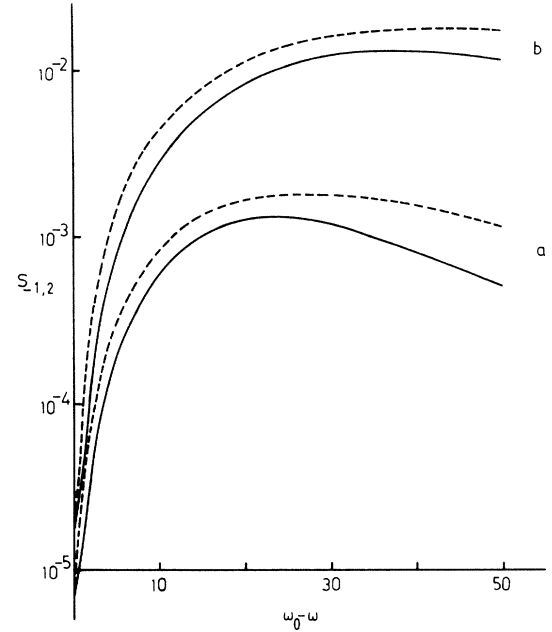


FIG. 4. Exact result for the degenerate four-wave-mixing signal as a function of detuning $\omega_0 - \omega$ when saturation effects are important. Curves *a* are for radiative relaxation and *b* are for collisional relaxation. Solid (dashed) curves correspond to field strengths $g_1 = 10$, $g_2 = 30$ ($g_1 = g_2 = 30$). For curves *b* the scale on *x* axis is twice that shown. Note the presence of saturation-induced hole at the line center.

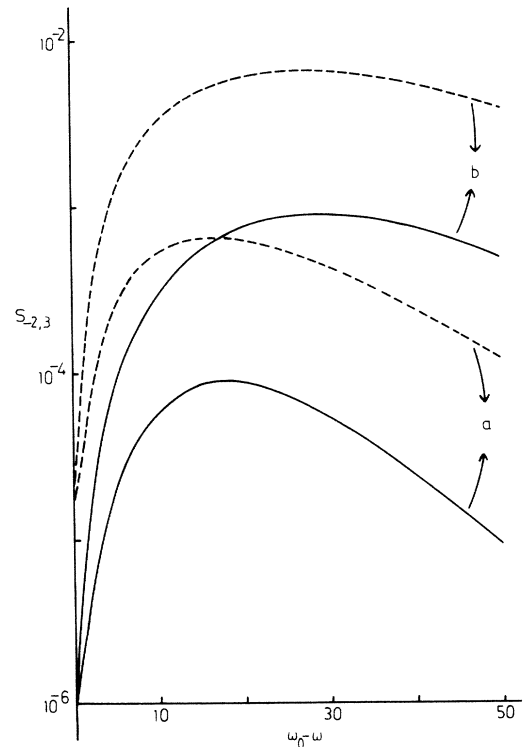


FIG. 5. Exact result for the degenerate six-wave-mixing signal as a function of $\omega_0 - \omega$. The labeling and parameters are same as in Fig. 4.

V. SATURATION AND COLLISIONAL EFFECTS IN NONLINEAR RESPONSE AT $2\omega_2 - \omega_1$

In this section we study various aspects of the response $R(2\omega_2 - \omega_1)$ at $2\omega_2 - \omega_1$ and in particular we discuss how the saturation of, say, one of the fields can affect such a response. From (2.12) we find that

$$R(2\omega_2 - \omega_1) = (\psi_1^{(1)})^* = \psi_2^{(-1)}, \quad (5.1)$$

From (2.19), $A_{-2}^{(0)} = 0$ and $A_{-1}^{(1)}$ is

$$A_{-1}^{(1)} = -2g_2 \left[\frac{1}{D_{-1}} + \frac{1}{D_0^*} \right] \eta \left[\frac{1}{T_1} + \frac{2g_2^2}{D_0^*} + \frac{2g_2^2}{D_0} \right]^{-1} \left[\frac{1}{T_1} + i\Omega + \frac{2g_2^2}{D_1^*} + \frac{2g_2^2}{D_{-1}} \right]^{-1}, \quad (5.4)$$

and hence the four-wave-mixing response at $2\omega_2 - \omega_1$ to lowest nonvanishing order in g_1 is

$$R^{(1,\infty)}(2\omega_2 - \omega_1) = 2ig_2^2 g_1 \eta \frac{1}{D_1^*} \left[\frac{1}{D_{-1}} + \frac{1}{D_0^*} \right] \left[\frac{1}{T_1} + \frac{2g_2^2}{D_0^*} + \frac{2g_2^2}{D_0} \right]^{-1} \left[\frac{1}{T_1} + i\Omega + \frac{2g_2^2}{D_1^*} + \frac{2g_2^2}{D_{-1}} \right]^{-1} + O(g_1^2). \quad (5.5)$$

The usual four-wave-mixing response valid up to lowest order in g_1 and g_2 , i.e., to order $g_2^2 g_1$ is obtained from (5.5) by setting $g_2 = 0$ in all the denominators in (5.5):

$$R^{(1,2)}(2\omega_2 - \omega_1) \approx 2ig_2^2 g_1 \eta T_1 \frac{\left[\frac{2}{T_2} + i\Omega \right] \left[\frac{1}{T_2} + i\Delta_2 + i\Omega \right]^{-1}}{\left[\frac{1}{T_1} + i\Omega \right] \left[\frac{1}{T_2} + i\Delta_2 \right] \left[\frac{1}{T_2} - i\Delta_2 + i\Omega \right]}. \quad (5.6)$$

The expression (5.6) leads to the well-known collisionally induced coherence^{19,20} at $\Omega = 0$. The saturation effects change the situation. Upon simplification (5.5) leads to

$$R^{(1,\infty)}(2\omega_2 - \omega_1) = \frac{2ig_2^2 g_1 \eta \left[\frac{2}{T_2} + i\Omega \right]}{\left[\frac{1}{T_2} + i\Delta_2 \right]} \times \left[\frac{1}{T_1} + \frac{2g_2^2}{D_0^*} + \frac{2g_2^2}{D_0} \right]^{-1} P_2^{-1}(i\Omega), \quad (5.7)$$

where

$$P_2(z) = \left[\frac{1}{T_1} + z \right] \left[\frac{1}{T_2} + i\Delta_2 + z \right] \left[\frac{1}{T_2} - i\Delta_2 + z \right] + 4g_2^2 \left[\frac{1}{T_2} + z \right]. \quad (5.8)$$

which in terms of the "inversion" X_n is equal to

$$R(2\omega_2 - \omega_1) = (-2ig_2 X_{-1} - 2ig_1 X_{-2}) / D_1^*. \quad (5.2)$$

We calculate R to first order in g_1 but to all orders in g_2 . Such a response will be denoted by $R^{(1,\infty)}$. On combining (2.14) and (5.2) we get

$$R^{(1,\infty)}(2\omega_2 - \omega_1) = (-2ig_2 g_1 A_{-1}^{(1)} - 2ig_1 A_{-2}^{(0)}) / D_1^*. \quad (5.3)$$

The polynomial $P_2(z)$ is precisely the polynomial that determines, for example, the spectrum of the resonance fluorescence from a two-level system in strong fields. Thus the four-wave-mixing signal (to order g_1^2) will exhibit the usual characteristics associated with the ac Stark effect. Note that the saturation effects can restore²⁷ the resonance at $\Omega = 0$ even in the absence of collisions. One can make an estimate of the relative importance of the various resonances in (5.7). For example, for $\Delta_2 = 0$, the resonance at $\Omega = 0$ has a peak height which is proportional to $4 / |1/T_1 T_2 + 4g_2^2|^2 \sim 1/4g_2^4$ for $g_2^2 \gg 1/T_1 T_2$, where as the height of the peak at $\Omega = 2g_2$ will be proportional to $1/4g_2^2 (1/T_1 + 1/T_2)^2$. Thus at resonance $\Delta_2 = 0$, the ratio of the heights of the side peak and the central peak will be $g_2^2 / (1/T_1 + 1/T_2)^2$, suggesting that the peaks at $\Omega = \pm 2g_2$ will be much more prominent.

We next compute the response $R(2\omega_2 - \omega_1)$ to lowest order in g_2 but to all orders in g_1 . From the structure of R , it is clear that we have to calculate $R(2\omega_2 - \omega_1)$ to second order in g_2 . We denote this response by $R^{(\infty,2)}$. We need X_{-1} (X_{-2}) to first (second) order in g_2 . In the notation of (2.14) we need $B_{-1}^{(1)}$ and $B_{-2}^{(2)}$. Equation (2.21) already gives $B_{-1}^{(1)}$. Equation (2.22) gives $B_{-2}^{(2)}$ as

$$B_{-2}^{(2)} = -(\alpha_{-2} + g_1^2 f_{-2})^{-1} g_1 \beta_{-2} B_{-1}^{(1)}. \quad (5.9)$$

Using (5.9), the response $R^{(\infty,2)}$ becomes

$$R^{(\infty,2)}(2\omega_2-\omega_1) = -\frac{2ig_2}{D_1^*} B_{-1}^{(1)} \left[1 - 2g_1^2 \left[\frac{1}{D_{-2}} + \frac{1}{D_1^*} \right] \left[\frac{1}{T_1} + 2i\Omega + \frac{2g_1^2}{D_{-3}} + \frac{2g_1^2}{D_1^*} \right]^{-1} \right]. \quad (5.10)$$

The response $R^{(\infty,2)}$ has a more complex structure than $R^{(1,\infty)}$. Thus the nonlinear response shows different types of saturation character with regard to the strength of the two fields. Using (2.23), we see that (5.10) contains the products of the polynomials $P_1(-i\Omega), P_1(-2i\Omega)$ and hence the response $R^{(\infty,2)}$ or the four-wave-mixing signal, to order g_2^4 but to all orders in g_1 , will show resonant structures at the Rabi frequency and at the subharmonic, i.e., $\frac{1}{2}$ of the Rabi frequency. In Figs. 6 and 7 we show the asymmetry of the four-wave-mixing signals $S(2\omega_2-\omega_1) \propto |R(2\omega_2-\omega_1)|^2$ with regard to the strength of the two fields.

VI. NONLINEAR RESPONSE AT $3\omega_2-2\omega_1$

We next calculate the response at $3\omega_2-2\omega_1$, which has been the subject of experimental study recently.^{2,15,16} In the usual susceptibility language, such a response is given by $\chi^{(5)}$. From (2.12) we have

$$R(3\omega_2-2\omega_1) = (\psi_1^{(2)})^* = \psi_2^{(-2)}, \quad (6.1)$$

which is equal to

$$R(3\omega_2-2\omega_1) = (-2ig_2X_{-2} - 2ig_1X_{-3})/D_2^*. \quad (6.2)$$

The lowest-order contribution to $R(3\omega_2-2\omega_1)$ is proportional to $g_2^3g_1^2$. In what follows we calculate $R^{(2,\infty)}$ to all orders in g_2 , but to lowest order in g_1 , so that the effects of the saturating field g_2 are included. Using the coupled equation (2.8) for X_n 's, we find that

$$X_{-3} = O(g_1^2), \quad (6.3)$$

whereas X_{-2} to second order in g_1 , i.e., $A_{-2}^{(2)}$ can be obtained from (2.19). The final result for $R^{(2,\infty)}(3\omega_2-2\omega_1)$, which is valid to all orders in g_2 but to only order g_1^2 in g_1 , is found to be

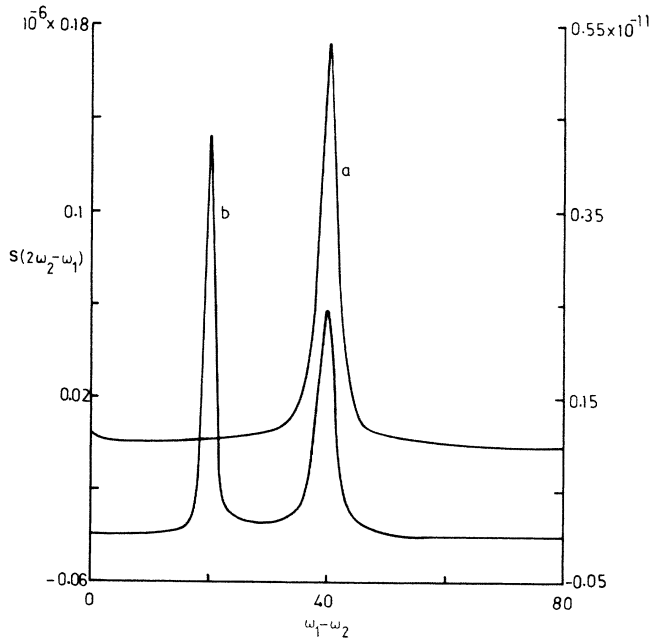


FIG. 6. Effect of saturation on the four-wave-mixing signal at $2\omega_2-\omega_1$ for radiative relaxation $1/T_2=1$, $1/T_1=2$. Curve a: field ω_1 weak ($g_1=0.1$) and field ω_2 strong ($g_2=20$). Curve b: field ω_2 weak ($g_2=0.1$) and field ω_1 strong ($g_1=20$). Frequency of the strong field is set at resonance with atomic frequency. Signal is scanned as a function of the frequency of the weak field. Vertical axis on the left is for the curve a, and vertical axis on right for curve b.

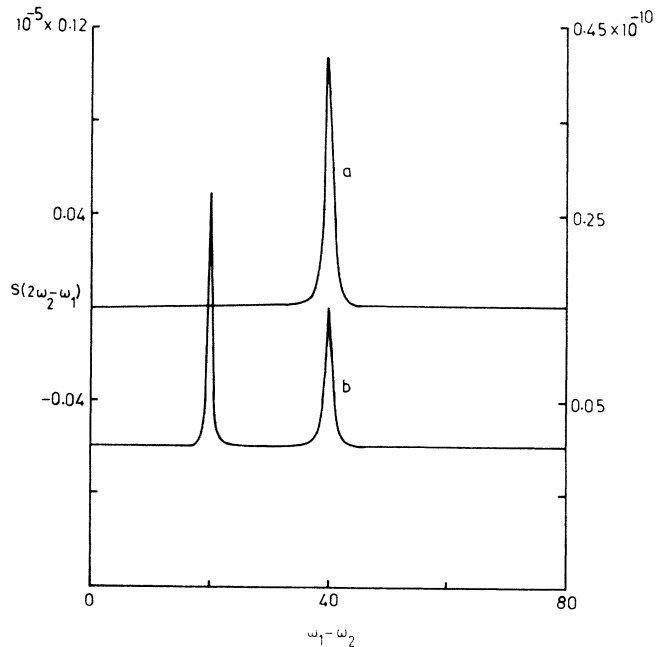


FIG. 7. Same as in Fig. 6 but for the collisional relaxation $1/T_2=10$, $1/T_1=2$. All frequencies are scaled in terms of $1/T_2$. The Y axis on the left corresponds to curve a and y axis on right is for curve b.

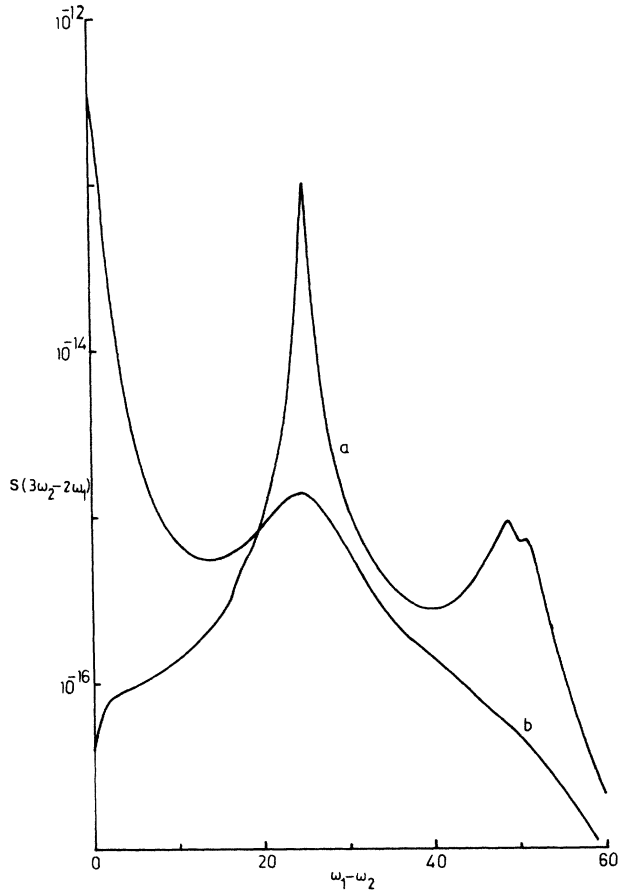


FIG. 8. Six-wave-mixing signal $\propto |R(3\omega_2 - 2\omega_1)|^2$ as a function of $\omega_1 - \omega_2$ for $\omega_0 - \omega_2 = 50$, $g_1 = g_2 = 1$, and for radiative relaxation (curve *a*) and collisional relaxation (curve *b*). Note the collisionally induced coherence at $\omega_1 = \omega_2$. The scale factor is same in both the cases and is equal to $1/T_2$ for radiative relaxation.

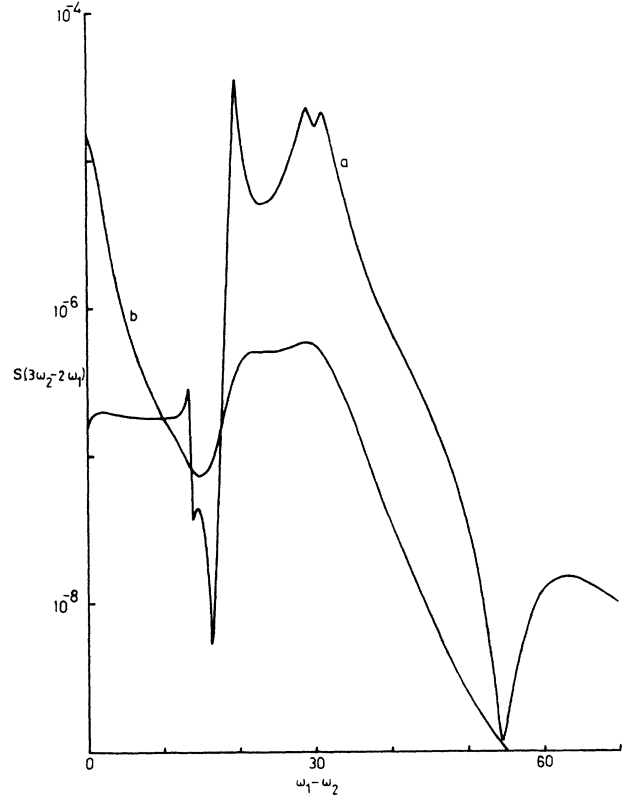


FIG. 9. Same as in Fig. 8, but for larger field strengths $g_1 = g_2 = 10$.

$$R(3\omega_2 - 2\omega_1) = -8i\eta g_1^2 g_2^3 \left[\frac{1}{T_1} + \frac{2g_2^2}{D_0} + \frac{2g_2^2}{D_0^*} \right]^{-1} P_2^{-1}(i\Omega) P_2^{-1}(2i\Omega) \\ \times \left[\frac{2}{T_2} + 3i\Omega \right] \left[\frac{2}{T_2} + i\Omega \right] \left[\frac{1}{T_2} + i\Delta_2 + 2i\Omega \right] \left[\frac{1}{T_2} + i\Delta_2 \right]^{-1}. \quad (6.4)$$

If saturation effects in g_2 are also ignored, then (6.4) reduces to

$$R(3\omega_2 - 2\omega_1) = -8i\eta g_1^2 g_2^3 T_1 \left[i\Omega + \frac{1}{T_1} \right]^{-1} \left[2i\Omega + \frac{1}{T_1} \right]^{-1} \left[\frac{1}{T_2} + i\Delta_2 \right]^{-1} \left[\frac{1}{T_2} + i\Delta_2 + i\Omega \right]^{-1} \\ \times \left[\frac{1}{T_2} - i\Delta_2 + i\Omega \right]^{-1} \left[\frac{1}{T_2} + i\Delta_2 + 2i\Omega \right]^{-1} \left[\frac{1}{T_2} - i\Delta_2 + 2i\Omega \right]^{-1} \left[\frac{2}{T_2} + i\Omega \right] \left[\frac{2}{T_2} + 3i\Omega \right]. \quad (6.5)$$

Thus $\chi^{(5)}$ or $R(3\omega_2 - 2\omega_1)$ will show resonances at

$$\Omega = \pm \Delta_2, 0, \frac{\Delta_2}{2}. \quad (6.6)$$

Note that if $1/T_1 = 2/T_2$, as is the case for radiative relaxation, then the resonance at $\Omega = 0$ will not be seen in the coherent signal ($\propto |R|^2$). This is because the factor

$$\left| \left[\frac{2}{T_2} + 2i\Omega \right]^{-1} \left[\frac{2}{T_2} + 3i\Omega \right] \right|^2$$

increases in the neighborhood of $\Omega = 0$. We have thus found in $\chi^{(5)}$ another example of collision-induced coherence. Figures 8 and 9 show the existence of the collision-induced coherence at $\Omega = 0$. Figure 8 also shows the appearance of the peaks as predicted by (6.6). A structure in

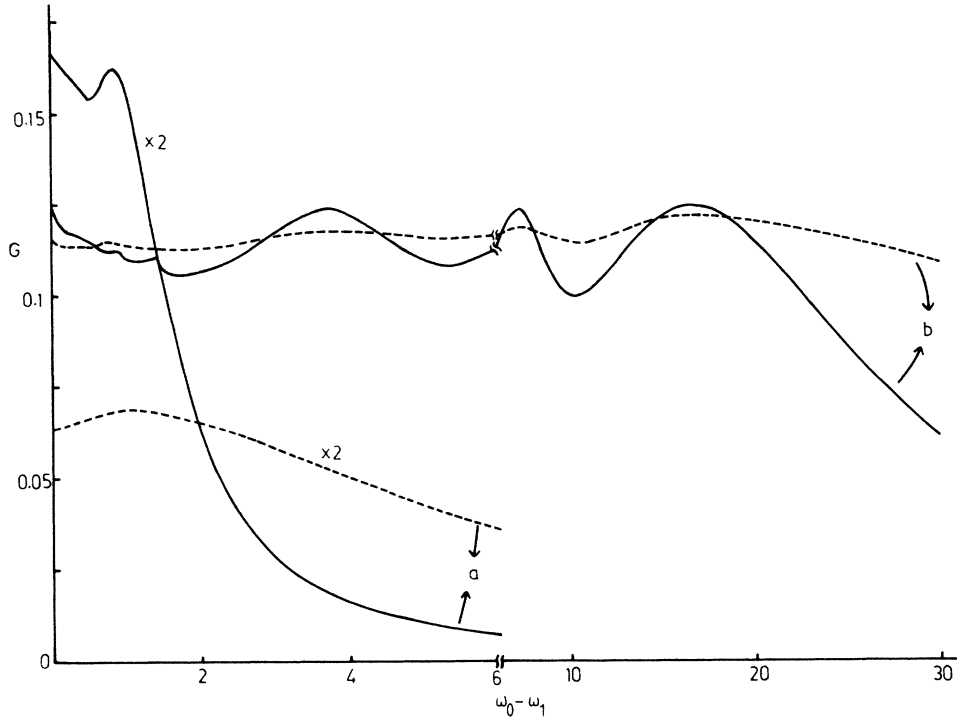


FIG. 10. Gain profile for two symmetrically displaced modes around line center as a function of the detuning from line center. Solid curves are for radiative relaxation, dashed curves represent collisional relaxation. Curve *a* is for moderate or weak $g_1 = g_2 = 1$ and curve *b* for strong $g_1 = g_2 = 10$ fields. The scale factor is same in both cases and hence for collisional relaxation, considerable power broadening is observed.

the resonance at $\Omega = 50$ is probably because the numerical result is obtained to all orders in g_1 and g_2 . Such complexities due to increased field strengths are more evident in Fig. 9 though g 's are smaller than Δ .

The full expression (6.4) for $R(3\omega_2 - 2\omega_1)$ shows the presence of ac Stark effect. In fact the response not only

shows the structures corresponding to the usual Rabi oscillations, but also shows structures at the subharmonic of the Rabi frequency with a width which is also reduced by a factor of 2. The present analysis shows how the successive higher-order susceptibilities exhibit more and more complex structure.

VII. INSTABILITIES IN HOMOGENEOUSLY BROADENED LASERS

Recently the instabilities in various types of laser systems have been extensively studied.^{17,28} In this section we show how the dynamical behavior of a two-level system in the presence of a bichromatic field can be used to understand some of these instabilities. Our dynamical equations of Sec. II contain the parameter η which will take positive values for inverted systems. One essentially examines the gain, of a given mode in the presence of say another mode, as a function of the strength of each mode. We have already seen in Sec. II and in Ref. 22 that the response $R(\omega_2)$ at the applied frequency has the following features: (1) In very weak fields g_1, g_2 , the response has a maximum at the line center $\omega_2 = \omega_0$; (2) for weak g_2 , but arbitrarily strong g_1 , the response exhibits Rabi structures at the Rabi frequency; and (3) as g_2 increases, the response $R(\omega_2)$ starts exhibiting new structures at the subharmonics of the new Rabi frequency. With further increase in g_2 , more and more subharmonics of the new Rabi frequency appear. In the experiments¹⁷ of Hillman *et al.*, the two-mode operation was observed. These modes were symmetrically placed around the line center.

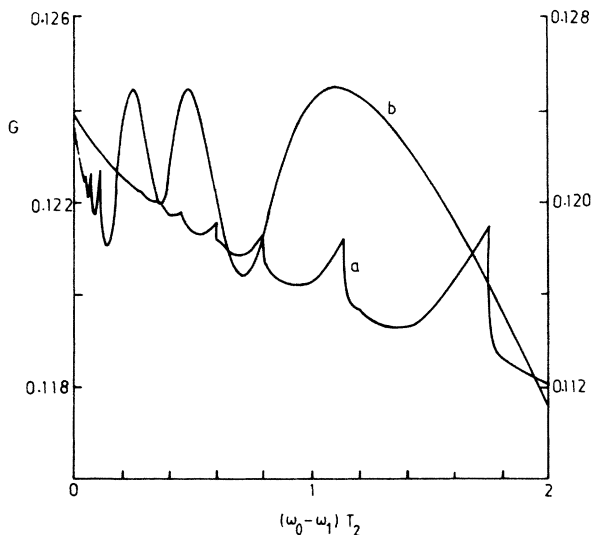


FIG. 11. Same as Fig. 10, but now the results in strong field for collisional relaxation are shown— $g_1 T_2 = g_2 T_2 = 10$, $T_2/T_1 = 0.2$. For *b*, the values on horizontal axis are 15 times of those shown.

The gain $G \propto \text{Im}R(\omega)$ can be obtained by setting $\omega_2 = \omega_0 + \delta$, $\omega_1 = \omega_0 - \delta$, and $g_1 = g_2$ in the equations of Sec. II. We have calculated such a gain for a range of parameters and the results are shown in Figs. 10 and 11. In Fig. 10, we show the gain profiles for moderate and large values of the Rabi frequency. For moderate values, only the main peak appears which is washed by increasing collisions in the system. For large field strengths, the gain profiles exhibit resonances at subharmonics of the Rabi frequency. This figure also shows the effect of increased collisions. With further increase of the driving field, additional subharmonics of the Rabi frequency can be seen. Hillman *et al.* have shown the existence of such subharmonics by analytic calculations in the case $T_1 = T_2$. Our numerical results enable one to study in detail the effect

of collisions. Note that in Fig. 10 we have used a different scaling, i.e., g_1 and g_2 are not in units of $1/T_2$; for example, for curve *c*, $g_1 T_2 = \frac{1}{10}$, whereas for curve *a*, $g_1 T_2 = 1$. This is done keeping in view the way in which one can perform the experiment. One can keep the field constant and add buffer gas to increase collisions. Gain profiles for the case when there are sufficient collisions and the fields are also strong are shown in Fig. 11.

ACKNOWLEDGMENTS

The authors are grateful to the Department of Science and Technology, Government of India for supporting this work.

- ¹S. Swain, *Advances in Atomic and Molecular Physics*, edited by D. R. Bates and B. Bederson (Academic, New York, 1980), Vol. 16, p. 159; P. L. Knight and P. W. Miloni, *Phys. Rep.* **66**, 21 (1980).
- ²S. A. Akhmanov, in *Nonlinear Spectroscopy*, edited by N. Bloembergen (North-Holland, Amsterdam, 1977), p. 239.
- ³J. H. Shirley, *Phys. Rev. A* **8**, 347 (1973); S. Haroche and F. Hartman, *ibid.* **6**, 1280 (1972).
- ⁴A. Compaan, E. Weiner-Avneer, and S. Chandra, *Phys. Rev. A* **17**, 1083 (1978).
- ⁵R. W. Boyd and S. Mukamel, *Phys. Rev. A* **29**, 1973 (1984).
- ⁶N. Bloembergen and Y. R. Shen, *Phys. Rev.* **133**, A37 (1964).
- ⁷B. R. Mollow, *Phys. Rev. A* **5**, 2217 (1972).
- ⁸B. R. Mollow, *Phys. Rev.* **188**, 1969 (1969).
- ⁹A. E. Kaplan, *Zh. Eksp. Teor. Fiz.* **68**, 823 (1975) [*Sov. Phys.—JETP* **41**, 409 (1976)].
- ¹⁰R. L. Abrams and R. C. Lind, *Opt. Lett.* **2**, 94 (1978); T. Fu and M. Sargent, *ibid.* **4**, 366 (1977); G. P. Agrawal, *Phys. Rev. A* **28**, 2286 (1983).
- ¹¹M. A. Kramer, R. W. Boyd, L. W. Hillman, and C. R. Stroud (unpublished).
- ¹²A. M. Bonch-Bruевич, S. G. Przhibelskii, V. A. Khodovoi, and N. A. Chigir, *Zh. Eksp. Teor. Phys.* **70**, 445 (1976) [*Sov. Phys.—JETP* **43**, 230 (1976)].
- ¹³R. Boyd and D. J. Harter, *IEEE J. Quantum Electron.* **QE-16**, 1126 (1980).
- ¹⁴F. Y. Wu, S. Ezekiel, M. Ducloy, and B. R. Mollow, *Phys. Rev. Lett.* **38**, 1077 (1977).
- ¹⁵N. Tan-no, K. Okhawara, and H. Inaba, *Phys. Rev. Lett.* **46**, 1282 (1981).
- ¹⁶R. K. Raj, Q. F. Gao, D. Bloch, and M. Ducloy, *Opt. Commun.* **51**, 117 (1984); D. Bloch and M. Ducloy, *J. Opt. Soc. Am.* **73**, 635 (1983).
- ¹⁷L. Hillman, J. Krasinski, R. W. Boyd, and C. R. Stroud, *Phys. Rev. Lett.* **52**, 1605 (1984).
- ¹⁸A. M. Bonch-Bruевич, S. G. Przhibelskii, and N. A. Chigir, *Zh. Eksp. Teor. Phys.* **80**, 565 (1981) [*Sov. Phys.—JETP* **53**, 285 (1981)]; A. M. Bonch-Bruевич, T. A. Vartanyan, and N. A. Chigir, *ibid.* **77**, 1899 (1979) [*ibid.* **50**, 901 (1979)]; G. I. Toptygina and E. E. Fradkin, *ibid.* **82**, 429 (1982) [*ibid.* **55**, 246 (1982)].
- ¹⁹N. Bloembergen, A. R. Bogdan, and M. W. Downer, in *Laser Spectroscopy V*, edited by A. R. W. McKellar, T. Oka, and B. P. Stoicheff (Springer, Berlin, 1981), p. 157; Y. Prior, A. R. Bogdan, M. Dagenais, and N. Bloembergen, *Phys. Rev. Lett.* **46**, 111 (1981).
- ²⁰G. Grynberg, *J. Phys. B* **14**, 2089 (1981); R. Scholz, J. Mlynek, and W. Lange, *Phys. Rev. Lett.* **51**, 1761 (1983).
- ²¹L. W. Hillman, R. W. Boyd, J. Krasinski, and C. R. Stroud, Jr., *Opt. Commun.* **45**, 416 (1983).
- ²²G. S. Agarwal and N. Nayak, *J. Opt. Soc. Am. B* **1**, 164 (1984).
- ²³The resonances at subharmonics of Rabi frequency also occur in absorption in strongly modulated intense fields [G. S. Agarwal and N. Nayak, *Phys. Rev. A* **31**, 3175 (1985)].
- ²⁴C. V. Heer and N. C. Griffin, *Opt. Lett.* **4**, 239 (1979).
- ²⁵If the two fields are acting on different transitions, then exact susceptibilities can be easily obtained. See, for example, G. P. Agrawal, *Phys. Rev. A* **29**, 994 (1984).
- ²⁶R. Saxena and G. S. Agarwal, *Opt. Commun.* **40**, 357 (1982).
- ²⁷See, for example, A. D. Wilson-Gordon, *Phys. Rev. A* **26**, 2768 (1982), for the calculation in the next order in perturbation g_2 .
- ²⁸R. S. Gioggia and N. B. Abraham, *Phys. Rev. Lett.* **51**, 650 (1983); L. W. Casperson, *Phys. Rev. A* **21**, 911 (1980); **23**, 248 (1981).